

LETTER TO THE EDITOR

The anti-glitching gamma-ray pulsar PSR J1522-5735

A.G. Panin ^{*} and E.V. Sokolova ^{**}

Institute for Nuclear Research of the Russian Academy of Sciences, Moscow 117312, Russia

Received <date> / Accepted <date>

ABSTRACT

Context. A small number of pulsar glitches have been identified as anti-glitches or spin-down glitches, where the overall contribution to the pulsar's rotation frequency is negative. A notable example of a spin-down glitch was observed in PSR 1522-5735, a radio-quiet gamma-ray pulsar discovered by blind searches in the 3-year data from the *Fermi* Large Area Telescope (LAT).

Aims. This work aims to search for PSR 1522-5735's glitches using *Fermi*-LAT data from over 15 years of observations.

Methods. The weighted H-test statistic was applied to identify glitches and evaluate the related changes in pulsar's spin parameters. The timing solution based on these results was further refined by maximization of the unbinned likelihood. The Bayesian information criterion was used to set an appropriate number of parameters in the timing solution to avoid overfitting.

Results. The analysis revealed eight glitch events: regular spin-up glitch, spin-up glitch over-recovered to a spin-down and six anti-glitches. These events were radiatively quiet, exhibiting no significant variations in the shape of the pulse profile or energy flux.

Conclusions. The results may suggest that an internal mechanism is responsible for spin-down glitch phenomena.

Key words. (Stars:) pulsars: general – (Stars:) pulsars: individual ...

1. Introduction

Pulsars are fast rotating neutron stars. Dipole radiation and particle winds cause pulsars to slow down extremely steadily making them amongst the most precise time measures in the Universe. Nevertheless, many pulsars exhibit sudden step-like increase of rotation frequency, known as glitches (Radhakrishnan & Manchester 1969; Reichley & Downs 1969; Espinoza et al. 2011). It is believed that glitches are associated with angular momentum transfer from faster rotating superfluid stellar interior to the neutron star crust (Anderson & Itoh 1975; Pines & Alpar 1985; Link et al. 1992).

Recent timing observations of the magnetar 1E 2259+586 by Archibald et al. (2013) revealed a sudden spin-down event, i.e. anti-glitch. The anti-glitch was accompanied by a hard X-ray burst detected by the *Fermi* Gamma-ray Burst Monitor (Foley et al. 2012) with a subsequent increase in the flux and a moderate change in the pulse profile (Archibald et al. 2013). However, the subsequent monitoring of the magnetar 1E 2259+586 led to the detection of another anti-glitch (Younes et al. 2020) with no evidence for flux enhancement or change in the spectral or pulse profile shape.

As of the present date, eight anti-glitches have been identified in a total of four pulsars (Archibald et al. 2013; Younes et al. 2020; Ray et al. 2019; Şaşmaz Muş et al. 2014; İçdem et al. 2012; Pintore et al. 2016; Vurgun et al. 2019; Tuo et al. 2024). Undoubtedly, the unexpected occurrence of anti-glitches poses a significant challenge to standard glitch theories. The close correlation observed between some anti-glitches and outburst activity suggest that these events may be due to the influence of external processes, such as strong outflows (Tong 2014), a sudden twisting of the magnetic field lines (Lyutikov 2013), or the accretion of orbiting objects (Katz 2014; Huang & Geng 2014). In

contrast, the identification of radiation-quiet anti-glitches suggests that their potential origin may be in the neutron star's interior (Duncan 2013; Ranea-Sandoval & García 2015; García & Ranea-Sandoval 2015; Kantor & Gusakov 2014). This possibility is also supported by the recent discovery of an anti-glitch in the the rotation-powered pulsar (Tuo et al. 2024).

The *Fermi* Large Area Telescope, continuously observing more than 290 gamma-ray pulsars (Smith et al. 2023), is a powerful tool for studying glitches (Sokolova & Panin 2022). An illustrative example is the pulsar PSR 1522-5735, which was uncovered by blind search in the LAT data spanning three years. The follow-up timing analysis of gamma-ray emissions from this pulsar revealed a glitch that resulted in a rapid decrease in the rotation frequency (Pletsch et al. 2013). In this paper, we report on the timing analysis of over 15 years of *Fermi*-LAT data for the pulsar PSR J1522-5735. We detected eight glitch events, six of which were categorized as anti-glitches.

The paper is organized as follows. *Fermi*-LAT data selection and preparation procedures are explained in Section 2. In Section 3 we introduce a phase model of pulsar rotation and identify glitches by using the H-test statistic. The timing method used to precise measure phase model parameters is detailed in Section 4. The resulting timing solution is presented in Section 5. In Section 6 we perform emission variability analysis. Finally, a summary is presented in Section 7.

2. Data preparation

The paper is based on the *Fermi*-LAT publicly available gamma-ray data for the time period from 2008 August 4 (54683 MJD) to 2024 April 5 (60405 MJD), which was prepared with *Fermi Science Tools* package version v11r5p3. For the analysis we included SOURCE-class photons according to the P8R3_SOURCE_V3 instrument response functions with the energies above 100 MeV, arrived within 5° region around the PSR

* E-mail: e-mail: panin@ms2.inr.ac.ru

** E-mail: e-mail: sokol1@ms2.inr.ac.ru

J1522-5735 position, with a zenith angle $< 100^\circ$, and when the LAT's rocking angle was $< 52^\circ$.

To increase sensitivity to pulsations, we calculated the weight w_i for each photon – the probability that the photon was emitted by the pulsar. We constructed spectral model of gamma-ray sources in the region around the PSR J1522-5735 that includes *Fermi*-LAT 4FGL sources (Ballet et al. 2023) in an 10° radius circle as well as galactic and isotropic diffuse emission components. The model parameters were optimized with binned likelihood analysis by the *gtlike* tool. The spectral parameters of the pulsar and all sources within 5° and the normalizations of the background models were free to vary in the fit. With the best-fitting source model, we used *gtsrcprob* to compute photons' weights based on their reconstructed energy and arrival direction. A total of 500000 photons with the highest weights were kept for the subsequent analysis. Finally, the photon arrival times are converted to barycentric frame using the *gtbary* tool. These computations were performed with the PSR J1522-5735's sky position constrained to high precision by Smith et al. (2023).

3. Glitch identification

The analysis of this and following sections employs the photon arrival times t_i and weights w_i by relating them to a certain rotational phase model. The model is usually given by a Taylor series expansion in time around a chosen reference epoch t_0 ,

$$\Phi(t) = \Phi_0 + f(t - t_0) + \frac{\dot{f}}{2}(t - t_0)^2 + \dots, \quad (1)$$

where f is pulsar frequency and \dot{f} denote frequency derivative over time.

As shown below the PSR J1522-5735 exhibited a sudden deviations from the model (1), which correspond to glitch events. A glitch accruing at time t_g with permanent change in pulsar frequency Δf_p and frequency time derivative $\Delta \dot{f}_p$ and with frequency increment Δf_d decaying exponentially on timescale τ_d causes a phase offset at time $t > t_g$ of

$$\Delta\Phi(t) = \Delta f_p(t - t_g) + \frac{\Delta \dot{f}_p}{2}(t - t_g)^2 + \dots + \Delta f_d \tau_d \left(1 - e^{-\frac{t-t_g}{\tau_d}}\right). \quad (2)$$

Note, that the instant changes in frequency and frequency derivative due to glitch are $\Delta f = \Delta f_p + \Delta f_d$ and $\Delta \dot{f} = \Delta \dot{f}_p - \Delta f_d / \tau_d$ respectively.

The presence of glitches significantly complicates the timing analysis. In order to identify them for PSR J1522-5735 and evaluate the spin-parameter changes associated with the glitches we applied the weighted H-test statistic (Kerr 2011). We divided the data spanning more than 15 years into 115-day data segments with 90% overlap. Then the value of H was computed separately for each segment,

$$H = \max_{1 \leq L \leq 20} \left[\sum_{l=1}^L |\alpha_l|^2 - 4(L - 1) \right], \quad (3)$$

where α_l is a Fourier amplitude of the l -th harmonic,

$$\alpha_l = \frac{1}{\kappa} \sum_i w_i e^{-il\Phi(t_i)}, \quad (4)$$

with the normalization constant,

$$\kappa^2 = \frac{1}{2} \sum_i w_i^2.$$

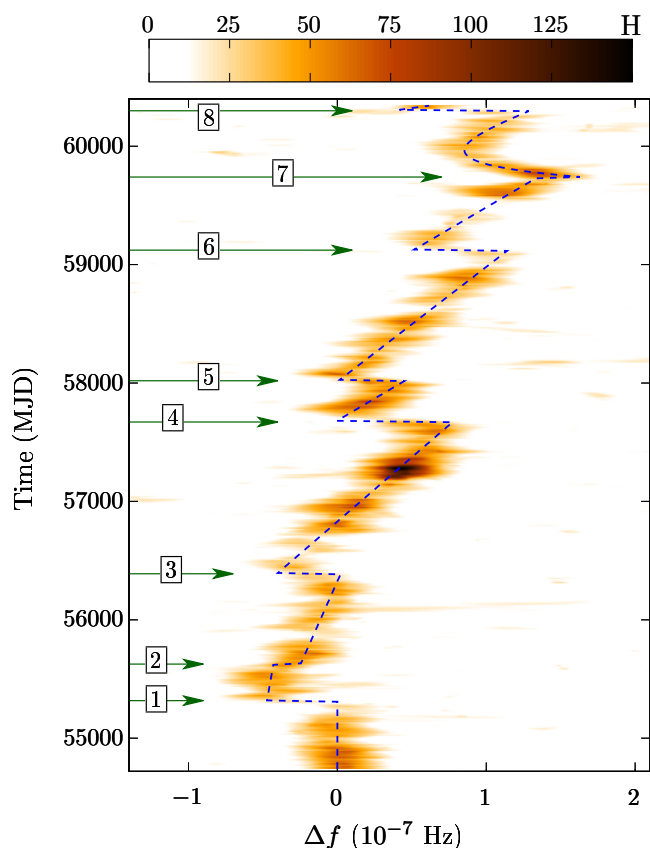


Fig. 1. The weighted H-test for PSR J1522-5735 calculated in 90% overlapping 115-day data segments, with the phase model (1), at fixed \dot{f} and over small range in f centered on the pre-glitch value. The vertical axis shows the time midpoint of the data segment. The horizontal axis shows the offset in f from the pre-glitch value. The weighted H-test is shown by the color-bar. The glitch events are noted by the arrows. The dashed blue curve is superimposed to show the timing solution, given in Table 1.

The phase of each photon in Eq. (4) was determined using pre-glitch phase model (1), in which we kept only the first two terms of the Taylor series expansion according to the timing solution of Smith et al. (2023). Then we fixed f and scanned range in f on a dense grid around given value. At each grid point we computed H using photons from the given data segment. The result is shown in the Figure 1.

The visual inspection of the weighted H-test plot revealed sudden changes of the pulsar's rotation rate around the epochs noted by the arrows in the Figure 1, which are candidates for glitches. From these results we estimated the values for the spin-parameter changes and glitch epochs which were refined by the timing procedure described in the following section.

4. Timing analysis

To accurately estimate the pulsar's rotational and glitch parameters we used the timing procedure proposed by Clark et al. (2017), based on unbinned likelihood maximization. The rotational phase Φ is a function of the photon arrival time t_i and a set of phase model parameters, see Eqs. (1), (2). For a template pulse profile $F(\Phi)$, which is an analytic approximation of a wrapped probability density function of the pulsar's rotational phase, the

Table 1. The inferred spin and glitches parameters of PSR J1522-5735.

| Parameter | Value |
|--|---|
| Right ascension, α (J2000.0) | $15^{\text{h}}22^{\text{m}}05.^{\text{s}}29$ |
| Declination, δ (J2000.0) | $-57^{\circ}34'58''.73$ |
| Epoch (MJD) | 57550 |
| Weighted H-test | 2157 |
| Spin frequency, f (Hz) | $4.895137036^{+3 \times 10^{-9}}_{-1 \times 10^{-9}}$ |
| Frequency derivative, \dot{f} (10^{-12} Hz/s) | $-1.49673^{+1 \times 10^{-5}}_{-1 \times 10^{-5}}$ |

| N | Epoch MJD | Δf_p 10^{-8} Hz | $\Delta \dot{f}_p$ 10^{-16} Hz/s | $\Delta \dot{f}_d$ 10^{-8} Hz | τ_d days |
|----|---------------------|------------------------------|---------------------------------------|------------------------------------|--------------------|
| g1 | 55317^{+3}_{-6} | $-4.7^{+0.4}_{-0.2}$ | 2^{+2}_{-3} | - | - |
| g2 | 55626^{+18}_{-13} | 1.8^{+4}_{-3} | 2^{+3}_{-2} | - | - |
| g3 | 56389^{+5}_{-5} | $-4.3^{+0.1}_{-0.1}$ | $6.6^{+0.3}_{-0.3}$ | - | - |
| g4 | 57671^{+3}_{-4} | $-7.9^{+0.3}_{-0.3}$ | 5^{+2}_{-2} | - | - |
| g5 | 58019^{+4}_{-5} | $-4.5^{+0.3}_{-0.3}$ | -4^{+2}_{-2} | - | - |
| g6 | 59122^{+4}_{-4} | $-6.4^{+0.2}_{-0.2}$ | $3.8^{+0.6}_{-0.6}$ | - | - |
| g7 | 59740^{+56}_{-25} | -12^{+2}_{-9} | 8^{+15}_{-4} | 15^{+8}_{-4} | 130^{+110}_{-23} |
| g8 | 60299^{+4}_{-4} | -9^{+1}_{-2} | 44^{+26}_{-24} | - | - |

Notes. The spin and glitches parameters correspond to the minimum of the BIC. Errors refer to the 68% confidence interval of the posterior marginalized distributions. Terms that do not contribute to a lower BIC are excluded from the phase model, their parameter values are indicated by dash.

likelihood is

$$\mathcal{L}(\lambda) = \prod_i [w_i F(\Phi(t_i, \lambda), \lambda) + (1 - w_i)], \quad (5)$$

where a set of phase model and template parameters are denoted by λ . The most likely values of λ are obtained by maximization of the likelihood (5), which is unbinned in both phase (via the template profile) and time. The advantage of this procedure is that there is no need to construct a set of data segments for pulse times of arrival (TOA) determination.

The Bayesian information criterion (Schwarz 1978) was used to select the model that best matches the data. It is defined as

$$\text{BIC} = -2 \log(\mathcal{L}(\lambda)) + k \log \left(\sum_{i=1}^N w_i \right), \quad (6)$$

where \mathcal{L} is the maximum likelihood calculated at the best-fitting parameters λ , k is the number of free parameters in the model. The latter accounts for the dimensionality penalty to avoid overfitting. When choosing between different models to describe the data, the one with minimum BIC is favoured.

At the beginning we constructed a template pulse profile based on the segment of the data before first glitch. With the pre-glitch spin parameters of the pulsar, f and \dot{f} , given by Smith et al. (2023), the phase for each photon was calculated according to Eq. (1). The weighted pulse profile was obtained by binning the phase and summing the photon weights in each phase bin. Based on these results we introduced a template pulse profile in the form of wrapped Gaussian peaks,

$$F(\Phi) = \left(1 - \sum_{\alpha} a_{\alpha} \right) + \sum_{\alpha} a_{\alpha} g(\Phi, \mu_{\alpha}, \sigma_{\alpha}). \quad (7)$$

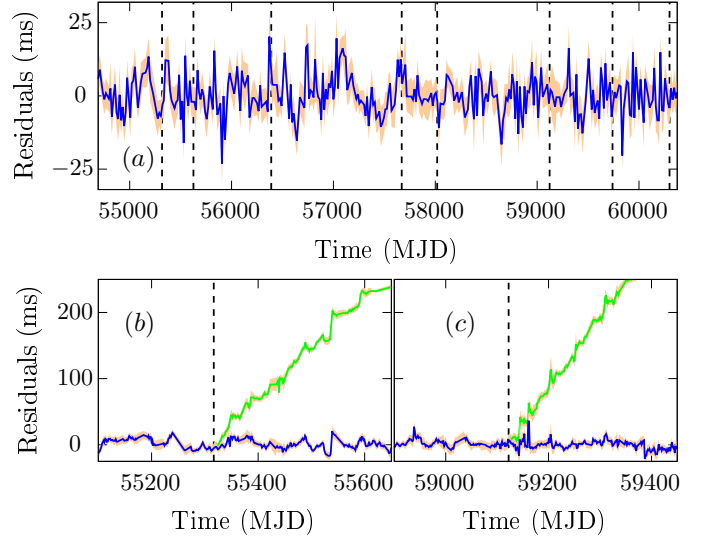


Fig. 2. Measured timing residuals from timing solutions fitted by unbinned likelihood maximization method. (a) Residuals between the best-fit timing solution given in Table 1 over the data span. (b) The same as (a), but around the epoch of the first glitch event (blue line), in comparison with residuals between pre-glitch model (green line). (c) The same as (a), but for the sixth glitch event. The shaded region correspond to one-sigma uncertainties.

Here $g(\Phi, \mu, \sigma)$ denotes a wrapped Gaussian peak centered at phase μ with width σ :

$$g(\Phi, \mu, \sigma) = \frac{1}{\sigma \sqrt{2\pi}} \sum_{k=-\infty}^{\infty} \exp \left(-\frac{(\Phi + k - \mu)^2}{2\sigma^2} \right). \quad (8)$$

The template was fitted to the weighted pulse profile by maximizing the likelihood. We used BIC to estimate the appropriate number of components to include in the template, finding that two Gaussian peaks were sufficient (see Figure 4).

Together with the template pulse profile parameters we then varied the spin parameters to find the most likely values that maximize the likelihood. To explore the likelihood surface in the parameter space, we used Markov Chain Monte Carlo sampling algorithm with parallel tempering, which demonstrates efficiency in multimodal sampling and optimization problems. At the final stage, we verified that inclusion \dot{f} did not improve the fit considerably according to the BIC.

The timing procedure outlined above was then used to refine the parameters of the glitches. We consistently expanded the data by including time intervals that covered the next glitches. The most likely glitch parameters were obtained by maximizing the likelihood. We added glitch parameters one by one, performed Monte Carlo likelihood maximization, and kept the new parameter in the phase model if its inclusion led to a decrease in the BIC. With the number of glitches parameters selected in this way, we performed a final longer Monte Carlo run, to obtain the value that maximizes the likelihood and uncertainty of each parameter.

5. Results

The results of the timing analysis confirmed the eight glitch events pointed out by the H-test. The minimum BIC timing solution is reported in Table 1 and also noted by the dashed curve in Figure 1. It includes six anti-glitches (events g1, g3, g4, g5,

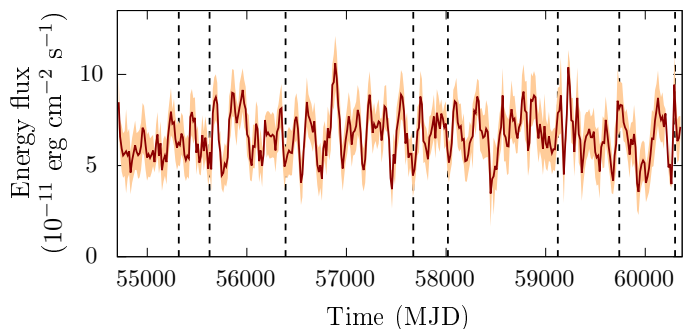


Fig. 3. The energy flux from PSR J1522-5735 calculated in 75% overlapping 60-day data segments. The horizontal axis shows the time midpoint of the data segment. The shaded region correspond to one-sigma uncertainties.

g6, g8 in Table 1) and two glitches (events g2, g7 in Table 1). An exponential post-glitch recovery terms for the anti-glitches and for the glitch g2 were disfavored by the BIC. For the glitch g7 the instant spin-up with $\Delta f_p + \Delta f_d > 0$ over-recovered to a net spin-down with $\Delta f_p < 0$.

In order to illustrate the validity of the phase model we measured the timing residuals — the difference between the model-predicted and the observed times of arrival (TOAs) of pulsar pulses. TOAs were obtained from maximum likelihood-based cross-correlation the photon phases within 15-days-long segments with the template pulse profile. The timing residuals are shown in Figure 2. Their smallness (Figure 2(a)) clearly certifies the phase-coherence of the timing solution. As one can see from the figure, the timing residuals exhibit continuous, low-level fluctuations caused by timing noise. In the Monte Carlo analysis discussed previously, we attempted to take these rotational irregularities into account by the glitch model (2). However, this did not lead to a lower BIC value. The residuals perturbed by the timing noise are clearly distinguishable from the PSR J1522-5735's glitches (see, for example, panels (b) and (c) of Figure 2), but the presence of timing noise can compromise the accuracy by which the glitch recoveries can be studied.

To assess whether the glitch events of PSR J1522-5735 are a regular spin-up glitches with fast over-recovery to a net spin-down state or an anti-glitches, the following Bayesian analysis was adopted. For each detected glitch event, we prepared a data segment that spans from 115 days before the glitch began to 30 days before the time of the next glitch. Then we performed a Monte Carlo runs within each data segment to explore parameter space of the glitches models with the decaying terms at fixed template pulse profile and pre-glitch parameters. Flat prior distributions for the free parameters within reasonably large intervals were used in the runs. The posterior distribution over $\Delta f_p + \Delta f_d$, which represents the instant change in the pulsar's frequency, for each glitch was obtained. By integrating these distributions over positive values we got an estimation for the likelihood that the models of a regular spin-up glitches with a certain amount of over-recovery to the spin-down describe these events. The results are 0.062 for the glitch events g1 and g8, 0.11 for g5 and > 0.15 for the others. Thus, the likelihood that the glitch events g1, g5 and g8 observed in PSR 1522-5735 represent a spin-up glitches appears to be marginal.

6. Pulse profile and energy flux

In order to search for pulse profile changes induced by the glitches, we performed Monte Carlo simulations similar to those

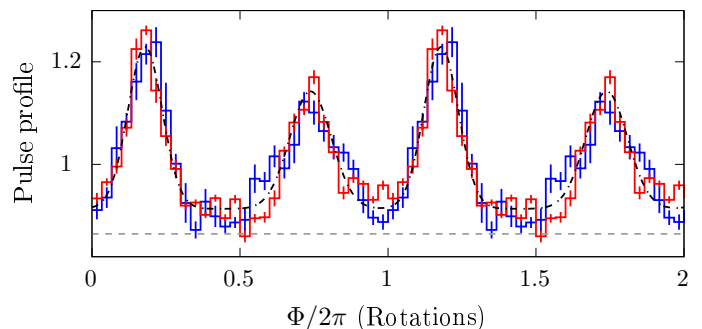


Fig. 4. Weighted pulse profiles of PSR J1522-5735 before the first (blue line) and after the third (red line) glitch events respectively. The error bars show one-sigma uncertainties. The average template pulse profiles used for timing analyses are shown by black dashed-dotted line. Grey dashed line indicates the background level.

previously described. We used the same data segments but permitted variation in the post-glitch pulse profile template during the runs. By "phase-folding" photon arrival times at each Monte Carlo step, the average weighted pulse profiles were calculated. We found no significant alteration in the pulse profile shape following either the spin-up or the spin-down glitches (see Figure 4).

It is also important to search for flux variations related to the glitches. For this purpose the gamma-ray flux from PSR 1522-5735 were monitored by dividing the full data into 60-day-long data segments with 75% overlap. Base on the data from each segment, we constructed the spectral model of the gamma-ray emission of the region around the PSR J1522-5735, as previously described in Section 2. The spectral parameters of the sources were fixed to the global ones due to the reduced exposure. The spectral normalization factors of PSR J1522-5735 and of the sources within 5° region around its position were set free and then optimized for every time segment with binned likelihood analysis by the *gtlike* tool. The energy flux calculated for each data segment is presented in Figure 3. As a result, we found no significant variations in the flux observed around the epochs of the glitch events.

7. Discussion

We carried out a comprehensive gamma-ray timing analysis of the pulsar PSR J1522-5735 using the publicly available *Fermi*-LAT data spanning from 2008 August 4 to 2024 April 5. The analysis revealed eight glitch events during this period: two spin-up glitches and six anti-glitches. The anti-glitches are well fitted by a model with step-like changes in frequency and frequency time derivative with no post-glitch recovery terms. However, a rapid recovery following anti-glitch within a few days cannot be reliably constrained due to the sparsity of gamma-ray data. On the other hand, the timescales for recoveries following these events are shorter than that of the majority of other glitches seen in rotation-powered pulsars, especially those characterized by a single exponential timescale.

The anti-glitch events were radiatively quiet, exhibiting no significant variations in the shape of the pulse profile or energy flux. This may suggest that an internal mechanism is responsible for these phenomena.

While this study was in the final stage, the paper by Zhou et al. (2024) appeared with similar results. In that work, TOAs fitting was used to ascertain glitch parameters, without employing BIC or alternative measures for model selection. This may

potentially clarify the differences in the glitch parameters found in this study and in the referenced paper, as some exceed 2-sigma level. Exploring these differences is beyond the scope of this paper and will be addressed in future studies.

Acknowledgements. We are indebted to O.E. Kalashev, G.I. Rubtsov and Y.V. Zhezher for numerous inspiring discussions. The work is supported by the Russian Science Foundation grant 17-72-20291. The numerical part of the work is performed at the cluster of the Theoretical Division of INR RAS.

References

- Anderson, P. W. & Itoh, N. 1975, *Nature*, 256, 25
 Archibald, R. F., Kaspi, V. M., Ng, C. Y., et al. 2013, *Nature*, 497, 591
 Ballet, J., Bruel, P., Burnett, T. H., & Lott, B. 2023
 Clark, C. J., Wu, J., Pletsch, H. J., et al. 2017, *ApJ*, 834, 106
 Şaşmaz Muş, S., Aydın, B., & Göğüş, E. 2014, *Mon. Not. Roy. Astron. Soc.*, 440, 2916
 Duncan, R. C. 2013, *Nature*, 497, 574
 Espinoza, C. M., Lyne, A. G., Stappers, B. W., & Kramer, M. 2011, *MNRAS*, 414, 1679
 Foley, S., Kouveliotou, C., Kaneko, Y., & Collazzi, A. 2012, *GRB Coordinates Network*, 13280, 1
 García, F. & Ranea-Sandoval, I. F. 2015, *Monthly Notices of the Royal Astronomical Society: Letters*, 449, L73
 Huang, Y. F. & Geng, J. J. 2014, *ApJ*, 782, L20
 İçdem, B., Baykal, A., & Inam, S. Ç. 2012, *MNRAS*, 419, 3109
 Kantor, E. M. & Gusakov, M. E. 2014, *The Astrophysical Journal Letters*, 797, L4
 Katz, J. I. 2014, *Ap&SS*, 349, 611
 Kerr, M. 2011, *ApJ*, 732, 38
 Link, B., Epstein, R. I., & van Riper, K. A. 1992, *Nature*, 359, 616
 Lyutikov, M. 2013, *arXiv e-prints*, arXiv:1306.2264
 Pines, D. & Alpar, M. A. 1985, *Nature*, 316, 27
 Pintore, F., Bernardini, F., Mereghetti, S., et al. 2016, *MNRAS*, 458, 2088
 Pletsch, H. J., Guillemot, L., Allen, B., et al. 2013, *ApJ*, 779, L11
 Radhakrishnan, V. & Manchester, R. N. 1969, *Nature*, 222, 228
 Ranea-Sandoval, I. F. & García, F. 2015, in *Compact Stars in the QCD Phase Diagram IV*
 Ray, P. S., Guillot, S., Ho, W. C. G., et al. 2019, *ApJ*, 879, 130
 Reichley, P. E. & Downs, G. S. 1969, *Nature*, 222, 229
 Schwarz, G. 1978, *The Annals of Statistics*, 6, 461
 Smith, D. A. et al. 2023, *Astrophys. J.*, 958, 191
 Sokolova, E. V. & Panin, A. G. 2022, *Astron. Astrophys.*, 660, A43
 Tong, H. 2014, *ApJ*, 784, 86
 Tuo, Y., Serim, M. M., Antonelli, M., et al. 2024, *Astrophys. J. Lett.*, 967, L13
 Vurgun, E., Chakraborty, M., Güver, T., & Göğüş, E. 2019, *New A*, 67, 45
 Younes, G., Ray, P. S., Baring, M. G., et al. 2020, *ApJ*, 896, L42
 Zhou, S. Q., Ye, W. T., Ge, M. Y., et al. 2024